Easy Come Easy Go: Surfaces Containing Immobilized Nanoparticles or Isolated Polycation Chains Facilitate Removal of Captured *Staphylococcus aureus* by Retarding Bacterial Bond Maturation

Bing Fang,[†] Ying Jiang,[‡] Vincent M. Rotello,[‡] Klaus Nüsslein,[§] and Maria M. Santore[†,*]

[†]Department of Polymer Science and Engineering, [‡]Department of Chemistry, and [§]Department of Microbiology, University of Massachusetts at Amherst, Amherst, Massachusetts 01003, United States

ABSTRACT Adhesion of bacteria is a key step in the functioning of antimicrobial surfaces or certain types of on-line sensors. The subsequent removal of these bacteria, within a ~10–30 min time frame, is equally important but complicated by the tendency of bacterial adhesion to strengthen within minutes of initial capture. This study uses *Staphylococcus aureus* as a model bacterium to demonstrate the general strategy of clustering adhesive surface functionality (at length scales smaller than the bacteria themselves) on otherwise nonadhesive surfaces to capture and retain bacteria (easy come) while limiting the progressive strengthening of adhesion. The loose attachment facilitates bacteria removal by moderate shearing flow (easy go). This strategy is demonstrated using surfaces containing sparsely and randomly arranged immobilized amine-functionalized nanoparticles or poly-L-lysine chains, about 10 nm in size. The rest of the surface is backfilled with a nonadhesive polyethylene glycol (PEG) brush that, by itself, repels *S. aureus*. The nanoparticles or polymer chains cluster cationic functionality, providing small regions that attract negatively charged *S. aureus* cells. Compared with surfaces of nearly uniform cationic character where *S. aureus* adhesion quickly becomes strong (on a time scale less than 5 min), placement of cationic charge in small clusters retards or prevents processes that increase bacteria adhesion on a time scale of ~30 min, providing "easy go" surfaces.

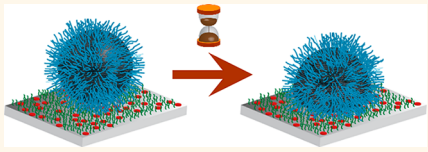

KEYWORDS: residence time dependence · contact time · charge cluster · immobilized nanoparticles · low fouling antimicrobial surfaces · surface heterogeneity · charge heterogeneity · polymer brush · immobilized nanoparticles · evolution of adhesion · interfacial relaxation · bacterial removal

The initial events of bacterial adhesion, which precede biofilm formation and facilitate bacterial retention on many surfaces, are usually governed by nonspecific long-range interactions such as van der Waals and electrostatic forces,[1−3] and are often reversible.[3−5] However, because bacteria−surface interactions strengthen with time,[4−7] removal of initially adhered bacteria becomes challenging. Even on negatively charged surfaces which should electrostatically repel bacteria, bacteria−surface bonds have been reported to strengthen within minutes of initial contact,[8] making bacterial removal from surfaces, ranging from biomedical devices to ship hulls, particularly vexing.

Research supports the idea that the physicochemical nature of the bacterial surfaces, which is responsible for initial capture, can also control the early stages (up to several tens of minutes) of interfacial restructuring and "bond maturation."[3,5,9−13] While only limited studies probe the time-evolution of bacterial adhesion strength, the investigations addressing this issue report a) that the growth of adhesion strength is a common behavior for many bacterial types and b) that adhesion is sensitive to surface chemistry. For instance, processes which occur within a few seconds to a minute after initial capture have been shown, for three *Streptococcus salivarius* strains, to affect the interfacial water[14] at the cell-surface gap. For

* Address correspondence to santore@mail.pse.umass.edu.

Received for review July 15, 2013 and accepted January 10, 2014.

Published online January 14, 2014
10.1021/nn405845y

substrate chemistries that undergo hydrogen bonding interactions, interactions increase on a time scale of minutes after the adsorption of several strains of *Staphylococcus epidermidus*.[8,15] Recent studies comparing AFM-driven bacterial disbonding, either from the tip itself (for *Streptococcus thermophilus*[4]) or from a substrate (for *Staphylococcus epidermidus* on the AFM cantilever[15]), reveal striking differences relative to flow-driven removal of adherent bacteria. In the AFM, stronger apparent adhesion (10^4–10^5 kT)[4] is thought to result from the closer contact forced by the AFM tip. By comparison, the adhesion of bacteria on glass and hydrophobic surfaces in quiescent and gentle-flow chambers (16–17 kT),[4] is associated with the secondary minimum.[15] Crossing from the primary to the secondary minimum is one possible physicochemical mechanism for increased adhesion following initial capture.[16] Separately, while the bacteria–surface contact areas involved in adhesion are not typically quantified, contact area is known to affect pull off force, for instance producing orders of magnitude differences when an AFM tip is pulled from a bacterium,[17] compared with removal of bacterium from a planar surface.[15] Bacterial deformation, were it to occur after initial contact, could increase adhesive interactions as the effective contact area progressively increases.[5]

The evolution of bacterial contact and adhesion is a particularly important issue for cationically functionalized surfaces that are used in contact antimicrobial materials[18–21] and could form the basis for capture-based on-line bacterial sensors and diagnostics. On "contact antimicrobial" surfaces, intimate bacteria–surface contact is essential[22–24] and killing correlates with adhesion;[5,25–27] however, studies have revealed how fouling and bacterial retention limits the utility of cationic surfaces.[19,26–30] The need for intimate contact between bacteria and killing surfaces, however, necessitates surface designs different from those in applications where bacteria adhesion might simply be avoided.[31]

Motivated by the challenge to create nonfouling contact (cationic) antimicrobial surfaces and capture-release surfaces for on-line bacterial sensors ("*easy come easy go*"), we explored bacterial adhesion kinetics, as distinct from capture kinetics, on surfaces with nanoscale clusters of adhesive cationic functionality. We pursued the unconventional strategy to engineer surfaces that facilitate bacterial capture but reduce the subsequent time-dependent increase in bacterial adhesion. By avoiding this increased adhesion after initial capture, slight increases in shear (or other small changes) can remove bacteria.

The key structural feature of the surfaces presented in this investigation is the clustering of cationic functionality at the nanoscale, conceptually different from classically uniform surfaces. Studies of this clustered motif and comparison to more uniform control surfaces provide fundamental insights into the kinetics of the adhesion process. Also it should be pointed out that our strategy of limiting adhesion to that occurring at short times is distinguished from the literature on chemical switching surfaces for bacterial release[32–36] where more substantial environmental changes or chemical regeneration is necessary.

This study uses *Staphylococcus aureus* as a model organism to demonstrate how surface architectures and distributions of nanoscale clusters of adhesive functionality on otherwise nonadhesive surfaces can be chosen to control the rate and extent of evolving bacterial adhesion after capture. In addition to documenting the influence of ionic strength on the evolution of *S. aureus* adhesion, the work highlights surfaces, containing a particular type of adhesive nanoscale feature, where *S. aureus* adhesion is arrested, *i.e.*, it does not continue to strengthen in the 30 min following initial capture. This inhibition favors more efficient removal of bacterial in simple shearing flows. While this study employs the cationic surface functionality used by antimicrobial applications, the focus here is on adhesion and bacterial removal. The antimicrobial activity of these surfaces will be addressed in a future work.

Technical Background and Rationale for Surface Designs. This study focuses on surfaces which contain cationically charged nanoscale objects or "nano-constructs." While the idea is general, in this study we separately used two cationic nanoconstructs, poly-L-lysine (PLL) chains and cationically functionalized gold nanoparticles. The PLL chains are relatively flat while the gold nanoparticles protrude ~8 nm from the substrate, allowing us to study the impact of the position of the positive charge relative to the substrate. The remainders of the surfaces are functionalized with end-tethered polyethlylene glycol (PEG) chains, forming a steric brush that repels bacteria. Indeed, without the cationic nanoconstructs on the surface, the PEG-brush architectures employed here completely repel bacteria over a wide range of conditions.[37–39] This ensures that the cationic PLL or nanoparticles are responsible for electrostatically capturing bacteria. As an additional benefit, the sparsely functionalized PLL surface in this project also repels proteins at the PLL densities employed in the current study.[40,41] This feature limits the interference of proteins with bacteria–surface interactions in potential applications. The uniform densely functionalized cationic control surfaces, in constrast, resemble cationic surfaces with strong antimicrobial action reported in the literature.[20,21]

Addressing the constraint requiring intimate bacteria–surface contact prior to removal, we designed experiments in which *S. aureus* are captured from gentle flow, as opposed to more prevalent experimental protocols in which bacteria settle onto a surface in quiescent conditions. In quiescent conditions, a thin

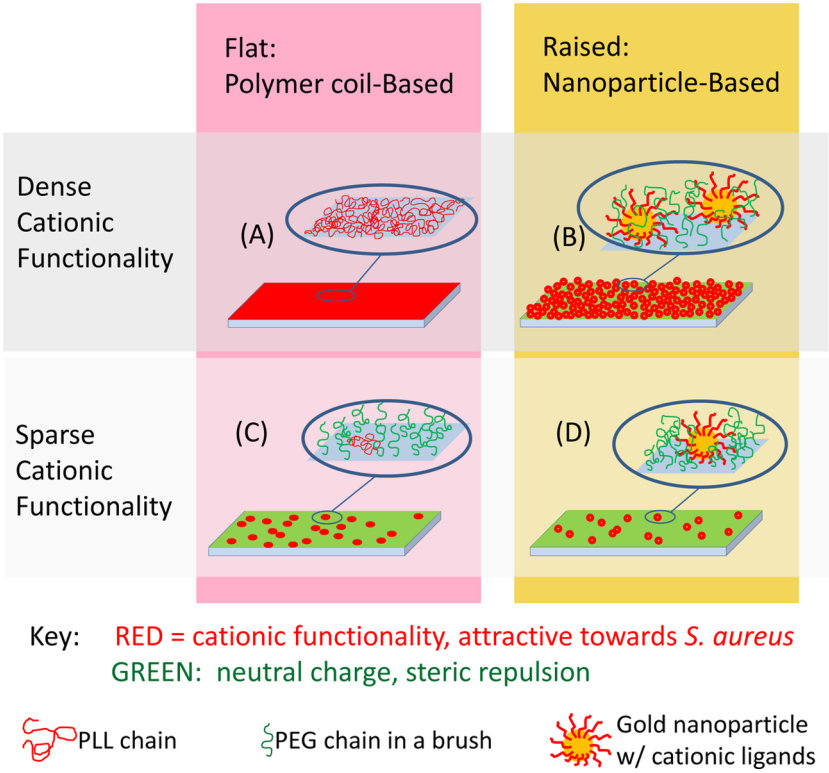

Figure 1. Schematics of the 4 surfaces employed in this work, with red indicating areas of cationic charge and green indicating a neutral PEG brush: (A) A saturated layer of PLL; (B) a dense layer (1000/μm^2) of cationically functionalized gold nanoparticles backfilled with a PEG brush; (C) a sparse layer of PLL coils (3500/μm^2) backfilled with a PEG brush; (D) a sparse layer of nanoparticles (400/μm^2) backfilled with a PEG brush.

layer of water may separate cells and surfaces or the cells may reside in a secondary minimum without molecular-scale contact.[4] Capture from flow ensures some minimal initial adhesion between the bacteria and the surface to overcome the hydrodynamic force at the wall, calculated from fundamentals for a 1-μm sphere near a wall in shear flow (22 s^{-1}) to be about 0.18 pN.[42]

This study considers the four surface designs, shown schematically in Figure 1, chosen from a larger surface library employed in extensive studies of bacterial capture.[37,38,42] The current study benchmarks sparse nanoconstructs against densely functionalized surfaces and raised adhesive nanoconstructs against more nearly flat ones. Using these systems, we can address the impact of charge clustering and the protrusion of these charge clusters from the substrate. These surfaces are based on our surface fabrication methods,[40] providing detailed characterization of the surfaces. These prior investigations also demonstrated retention of surface nanoconstructs and their functional activity after drying, or exposure to solvents, proteins, sonication, and a range of ionic strengths. The previous works also firmly established that the initial bacterial capture on these surfaces was controlled by electrostatic attractions.[37,38] The current study relies on this prior work to identify which surface compositions are able to capture and hold substantial numbers of *S. aureus* bacteria, several hundred within the field of view necessary for probing the subsequent growth of adhesion. The current study focuses on low densities of adhesive functionality balanced against sufficient adhesive driving force to capture *S. aureus* quickly and semipermanently in modest flow (corresponding to a wall shear rates of 20 s^{-1}).

For the two different cationic nanoconstructs, poly-L-lysine (PLL) chains and ~10 nm cationically functionalized gold nanoparticles, Figure 2 recapitulates, from our prior work,[37,38] the *S. aureus* capture rates as a function of the surface loading of cationic nanoconstructs within a PEG brush (which backfills the remaining surface.) The *S. aureus* capture rates on the *y*-axis of Figure 2 are normalized on the maximum transport-limited capture rate for bacterial suspensions having concentrations near 5 $\times$ 10^5/mL. Figure 2 contains the implicit control study where no bacteria adhere to surfaces bearing PEG brushes without PLL coils or nanoparticles.

The feature of Figure 2 germane to our current choice of surfaces is the presence of thresholds in the loadings of cationic nanoconstructs needed for bacterial capture. The surfaces with the smallest densities of PLL coils or cationic nanoparticles are unable to adhesively capture bacteria from gentle flow and are inappropriate to probe bacterial removal. Studies of bacterial removal must employ collector compositions

sufficiently above the adhesion thresholds to enable substantial numbers of bacteria to be captured relatively quickly, within minutes. Subsequent removal studies are most meaningful when the time scale for bacterial capture (inversely proportional to the capture rates on the *y*-axis of Figure 2) is shorter than the bacterial aging time. The sparse surfaces for nanoparticle and polymer coil cationic nanoconstructs were therefore chosen to be 400 np/μm^2 and 3500 chains/μm^2, both of which are appropriately greater than their respective thresholds. This gives sufficient *S. aureus* accumulation for studies of bacterial removal. The properties of these sparse surfaces are summarized in Table 1 and compared with the more densely cationic surfaces of each type: surfaces containing 1000 cationic nanoparticles/μm^2 and a saturated adsorbed layer of PLL (which contains 12 000 PLL chains/μm^2).

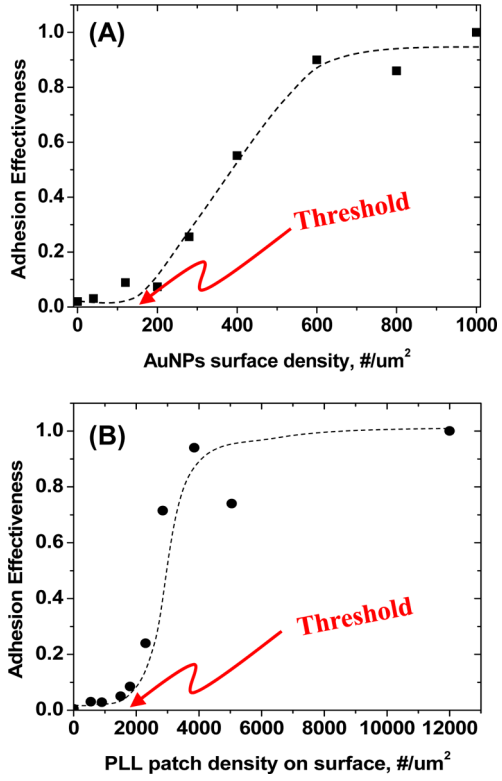

Figure 2. Adhesion efficiency of *S. aureus* on (A) nanoparticle-containing and (B) PLL-containing surfaces, from buffer with a Debye length of 2 nm.

In Table 1, key features of the sparsely functionalized surface include their modest net negative zeta potentials: this ensures that attractive interactions are localized at the positions of the cationic PLL and nanoparticle constructs. The remainder of the surface not only presents a sterically repulsive PEG brush, but sustains a net negative charge beneath the brush,[43] also repulsive to negative bacteria.

Another interesting feature in Table 1 is the average density of positive adhesive charge. This estimate was calculated based on the properties of the nanoconstructs described in the experimental section and knowledge of their surface loadings. Not all the amine groups may be charged, they may not all be accessible (for instance the charges beneath the nanoparticles would not be felt by approaching bacteria), and they may be reduced by counterion condensation. Nonetheless, Table 1 presents a first estimate and highlights the greater cationic charge on the PLL-constructs containing surfaces compared with the respective nanoparticle-containing surfaces.

While it might seem desirable to design a study that compares surfaces with fixed overall charge, presented differently on the different nanoconstructs, this goal turns out to be impractical because the different presentations of charge dominate the overall charge effects. In many cases, for instance, *S. aureus* do not adhere to what would be obvious choices for "control" surfaces (of uniform charge distribution) complementary to surfaces bearing low levels of clustered charge. In other instances, larger amounts of charge on the PLL coils buried inside or beneath the brush are substantially less adhesive than the cationic charge of the nanoparticles, making a comparison at fixed charge uninteresting. Our approach of choosing sparse surfaces as close to the respective adhesion thresholds as practical, but sufficiently above the thresholds to facilitate bacterial capture, provides a means to compare surfaces with similar overall initial adhesion at the time of capture. With this initial adhesion more nearly fixed, then the impact of surface design on the development of further *S. aureus*−surface bonds was investigated.

TABLE 1. Properties of Surfaces

adhesive nanoconstruct	saturated PLL coils	sparse PLL coils	saturated nanoparticles	sparse nanoparticles	plain PEG brush
Surface Density, #/μm^2	12000	3500	1000	400	0
Average spacing, nm	-	17	32	50	-
Overall PLL-PEG content, mg/m^2	0	0.61	0.3	0.67	1.1
Zeta Potential, mV*					
κ^{-1} = 1 nm	2 ± 5	- 12 ± 2	−19 ± 5	−22 ± 3	−17
κ^{-1} = 2 nm	6 ± 2	- 20 ± 3	−20 ± 4	−27 ± 3	−27
κ^{-1} = 4 nm	4 ± 2	- 23 ± 4	−30 ± 3	−37 ± 3	−30
Averaged density of positive charge, #/μm^2	1.4 × 10^6	4.2 × 10^5	2.0 × 10^5	8.0 × 10^4	-

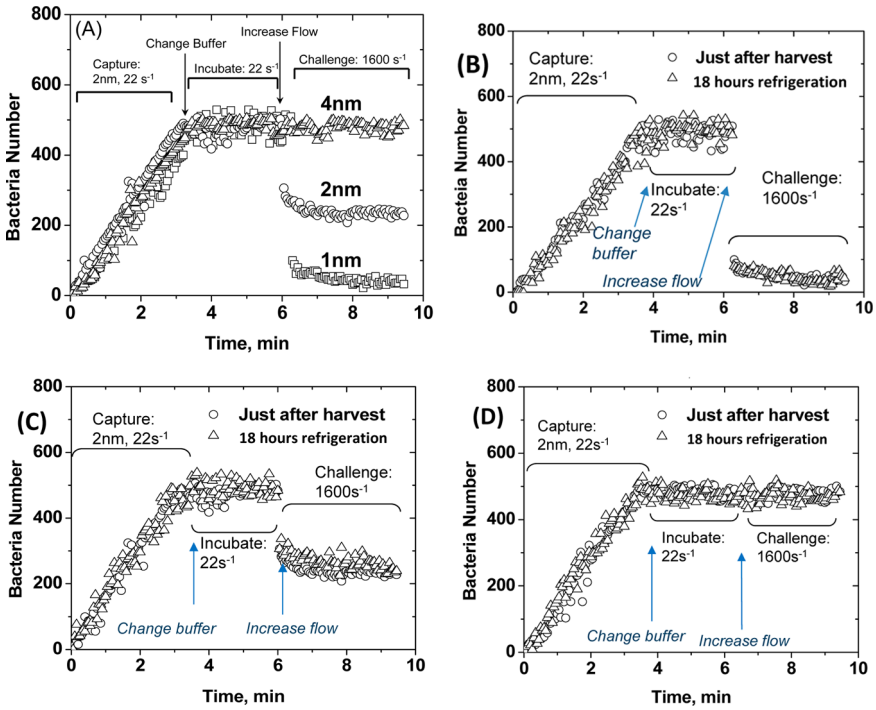

Figure 3. (A) Typical runs showing *S. aureus* capture, aging, and shear challenge, for example, on surfaces containing 3500 PLL chains /μm^2. The nominal surface residence time here is 5 min. (B–D) Runs comparing fresh *S. aureus* cells to those refrigerated 18 h prior to study. Each run includes caputure, aging, and shear challenge on surfaces containing 3500 PLL chains /μm^2. The nominal surface residence time here is 5 min. Incubation and challenge at different Debye lengths (B, 1 nm; C, 2 nm; D, 4 nm) spans the range of bacterial retention behaviors observed.

Also regarding the goal to create capture–release or "*easy come, easy go*" surfaces, the practical metric of bacterial retention in flow, rather than microbiological methods, was used to assess the evolving bacterial adhesion strength. This approach follows evidence that, on other surfaces, adhesive strengthening on time scales of tens of minutes may not require metabolic changes in bacteria.[3,9–13] Such changes may or may not occur in the *S. aureus* studied here, regardless of successful surface performance in terms of controlled adhesion. Microbiological assessment of bacterial features, for instance at longer times, is beyond the current scope.

RESULTS

Bacterial Removal at Elevated Shear. Bacteria were deposited from gently flowing buffer (at a wall shear rate of 22 s^{-1}, having an ionic strength of 0.026 M and a Debye length of κ^{-1} = 2 nm), incubated at the ionic strength of choice for a controlled period of time, and then challenged at the elevated wall shear rate, 1600 s^{-1}. Figure 3 shows an example for three sparse PLL surfaces. In the case of the nominal "5 minute" surface residence period shown in Figure 3A, the bacteria were aged in test buffer for 3 min prior to the high shear challenge, to give an average surface residence time (including a portion of the deposition process) near 5 min. For longer nominal aging periods of 15 and 30 min in other runs, the aging time was substantially longer than the deposition period so that the nominal times represented the aging times to within 10%.

Figure 3A illustrates key features of *S. aureus* removal from the patchy PLL brush. Importantly, bacteria removal is fast once the shear is increased, and the remaining bacteria are retained, indefinitely for practical purposes. We found no long-term bacterial loss in extended flow, up to 0.5 h wall shear rates of 1600 s^{-1}. The rapid bacterial removal rates, in Figure 3A, were characteristic of all runs, preventing a quantitative assessment of the disbonding rate. Because *S. aureus* that are removed at a wall shear rate of 1600 s^{-1} come off so quickly while the retained population is stable, reporting the size of the retained population (relative to the original) is meaningful.

Figure 3B–D show example runs comparing the behavior of fresh bacteria used in a particular adhesion run to a repeat run for the same conditions (choice of surface, ionic strength, surface residence time), but older bacteria (the last run for a particular bacterial batch). Figure 3B–D demonstrates that the test runs with two different ages of bacteria, within the range studied, are nearly indistinguishable, for the three examples shown, which (as Figure 4 will show) are the runs with the greatest sensitivity to ionic strength, where there is the greatest need for precision in distinguishing the retained and removed populations. This reproducibility is typical of all the runs and test conditions examined in this work.

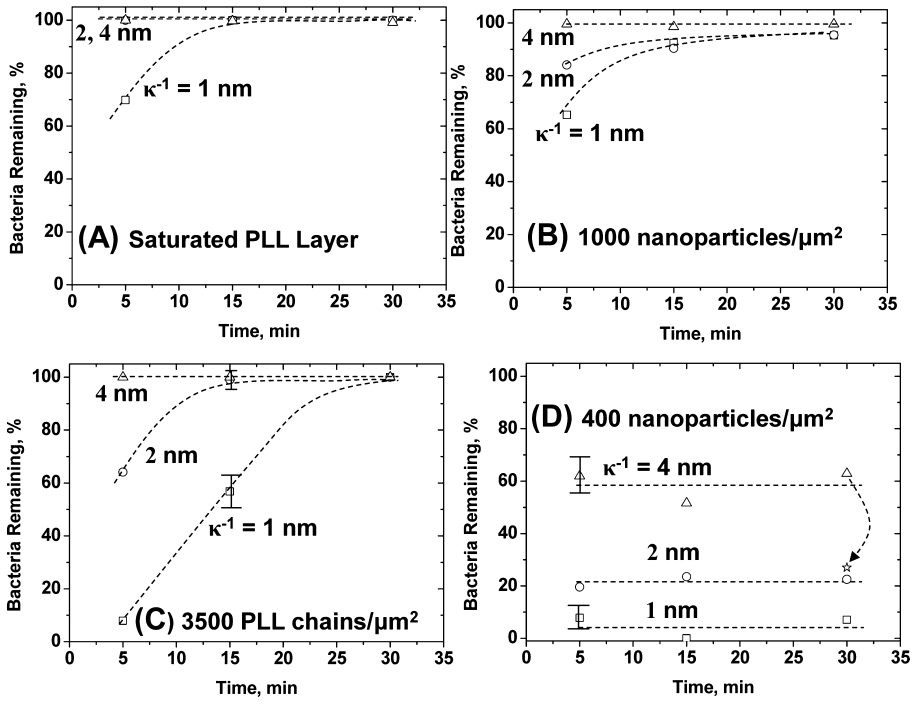

Figure 4. Summary of bacterial retention after shear challenge on different surfaces: (A) A saturated PLL layer; (B) a PEG brush containing 1000 nanoparticles/μm^2, (C) a PEG brush containing 3500 PLL coils/μm^2, and (D) a PEG brush containing 400 nanoparticles/μm^2. Symbols represent aging and shear challenge in buffers having different Debye lengths: triangles, 4 nm; circles 2 nm; squares 1 nm. The star in panel D is for a run aged in 4 nm buffer but challenged in 1 nm buffer. Typical error bars are shown and dashed lines guide the eye.

Figure 4 summarizes the sizes of the retained *S. aureus* populations, like those in Figure 3, as a function of surface residence time for different surfaces and ionic strengths during the aging period. In Figure 4A for saturated PLL surfaces, *S. aureus* adhesion is immediately strong, exceeding the pull-off-shear force of 12.8 pN, corresponding to shear flow of 1600 s^{-1} past a 1 μm sphere.[44] The results are mostly independent of ionic strength with the exception of the 5-min aging run in the buffer having κ^{-1} = 1 nm, where a weaker adhesion is found within the first 5 min. Within the next 10 min, however, the adhesion strength increases to the point of maximum pull-off strength in our experiments. In the case of surfaces containing 1000 nanoparticles/μm^2 in Figure 4B, a slight effect of residence time on adhesion is found: adhesion grows to (and beyond) forces of 12.8 pN in a ~20 min period, with faster adhesive development at low ionic strength. These observations of strong bonding are consistent with other reports[4,6,7,14] of strong bacteria–surface adhesion, fast development of bacteria–surface bonds, and the fouling problems on surfaces of relatively uniform cationic functionality.

Different behavior is found for the sparsely cationic surfaces. In the case of 3500 PLL patches/μm^2 in Figure 4C, *S. aureus* subject to aging in buffer having κ^{-1} = 4 nm (giving the strongest electrostatic attractions) became strongly bound within the first few minutes of capture. At higher ionic strength during aging and shear challenge, the effect of aging time is conspicuous: not only do weaker electrostatic attractions give weaker overall *S. aureus* binding, but processes that increase adhesion are slowed when the electrostatic attractions are made shorter range. This demonstrates that electrostatic interactions drive the adhesive tightening of bacteria to these surfaces.

More interesting still is the adhesion of bacteria on sparsely distributed nanoparticles in Figure 4D. In this case the development of adhesion is arrested early, and at a level that depends on ionic strength: bacteria are more completely removed at high ionic strength. However, the number of bacteria that are removed by 12.8 pN force is low and does not grow in time. The "locking in" of low adhesion strength for a substantial time window is a new behavior not seen previously and presumably attributed to the low cationic charge and its tightly clustered distribution on the sparse nanoparticle surfaces.

Bonding Extent *versus* Strength. In the main part of this study (following the protocol of Figure 3), both the aging of captured bacteria and the shear challenge were conducted at the same ionic strengths. Since the electrostatic interaction at a given time depends on ionic strength, it is worth decoupling the influence of salt on interfacial evolution (aging) from its impact on "bond strength" at the time of shear challenge. The distinction is unimportant in cases when adhesion is so

strong that an influence of ionic strength cannot be discerned, for instance on densely cationic surfaces (Figure 4A,B). When ionic strength is found to reduce bacterial retention (for instance at short times in Figure 4C or more generally in Figure 4D), we would like to learn if aging at different ionic strengths causes different structural evolutions of the bacteria–surface interfaces, or if observations merely result from differences in electrostatic interactions at the time of shear challenge.

Decoupling the influence of salt on aging from that on *S. aureus* removal requires a switch in buffer just prior to shear challenge, to uniform ionic conditions for bacterial removal (for instance arbitrarily choosing to conduct all shear challenges at a Debye length of 1 nm). Such a protocol was not possible for runs with 5 min aging times, because about 3 additional minutes are needed to switch to the buffer conditions for shear challenge. We therefore studied the impact of buffer choice during the shear challenge of longer experiments, focusing on the surface and aging conditions where this would be most conspicuous: a substrate with sparse nanoparticles with bacterial aging in κ^{-1} = 4 nm buffer. Here an additional set of runs involved aging in 4 nm buffer for 30 min and then switching back to 1 nm buffer for the shear challenge, averaged to give the star datum in Figure 4D.

For a given choice of surface and aging conditions, one expects a lower adhesion strength and fewer retained bacteria following a shear challenge in 1 nm buffer compared to that in 4 nm buffer. This expectation follows from the shorter range of electrostatic interactions during challenge in 1 nm buffer. The expectation is confirmed by the star datum in Figure 4D compared with the triangle at the same aging time. Importantly, however, the star for aging in 4 nm buffer lies above the square for aging in 1 nm buffer (with both shear challenges in 1 nm buffer conditions). Therefore, this test demonstrates that even when the Debye length is consistently set at low level during shear challenge, the aging rate (increasing adhesion) increases with Debye length during aging. In other words, independent of conditions during shear challenge, the structure of the bacteria–surface interface evolves more rapidly (to strengthen adhesion) in 4 nm buffer than it does in 1 nm buffer.

DISCUSSION

Electrostatically Driven Growth of Adhesion. While *S. aureus* adhesion on substantially cationic surfaces rapidly increases to levels exceeding those that can be measured with hydrodynamic pull-off experiments (resisting 12.8 pN within less than 5 min of initial capture), the two-step nature of bacterial adhesion from flow[3] is evident on surfaces with sparse cationic functionality. In the tens of minutes following capture on surfaces containing 3500 PLL coils/μm^2 in a PEG brush, bacteria become increasingly resistant to removal. On the most sparsely cationic surfaces (400 nanoparticles/μm^2), however, adhesion strength remains arrested near its low initial level. In particular on the sparse PLL surfaces, the influence of ionic strength on the evolution of adhesion after initial capture supports a mechanism of electrostatically driven "tightening" of the bacteria onto the surface. This adhesive tightening need not involve "living processes" or bacteria metabolism.[5]

Surface Design Parameters: Charge Density, Presentation, and Clustering. The results with the four different surface designs demonstrate that lower overall charge density (in Table 1) is associated with slower growth of bacterial adhesion, consistent with electrostatic-driven increases in adhesion after bacteria capture. Positioning charge in nanoscale clusters may also be important, although the relative importance of overall charge density *versus* clustering is complex. Clustering is certainly critical to the ability of surfaces with low adhesive functionality to capture bacteria at all (in Figure 2): more uniform distribution of the same numbers of cationic charges on equivalent surfaces will fail to capture round negative objects compared with clustered cationic charge on a collector.[45,46] For our system, a surface having the same numbers of cationic charges as the 400 np/μm^2 surface, but distributed uniformly or placed on ~400 PLL coils, will fail to capture bacteria at the conditions in this study. Therefore, with a practical goal of adhering and then releasing bacteria, the clustered charge presentation is a key design consideration: while low charge may facilitate bacterial release by limiting the ultimate adhesion, charge clustering facilitates *S. aureus* capture on these surfaces of extremely low overall charge. Charge presentation, within or at the brush periphery, is an additional consideration. The mechanistic roles of charge presentation, density, and clustering are discussed in more detail below.

Local Rearrangements. A first potential mechanism, in Figure 5A, for the increased bacteria adhesion with time is that negatively charged bacterial structures move closer to cationic surface nanoconstructs in the region of *S. aureus*–surface contact, possibly pushing against and deforming the PEG brush in doing so. Compression and small lateral motions of the PEG chains and bacteria surface molecules could be particularly important on surfaces with buried PLL patches, in contrast to the more accessible cationic nanoparticles. An important point, the local rearrangements on the sparse PLL surfaces might ultimately increase the effective contact area; however, we distinguish the "local rearrangement" mechanism as being *driven* by nanometer-scale electrostatic attractions within the *existing* bacteria–surface contact region. Thus, the strengthening of bacterial adhesion by local rearrangements could result in, but does not require, bacterial deformation. Nanometer scale mobility of polymeric

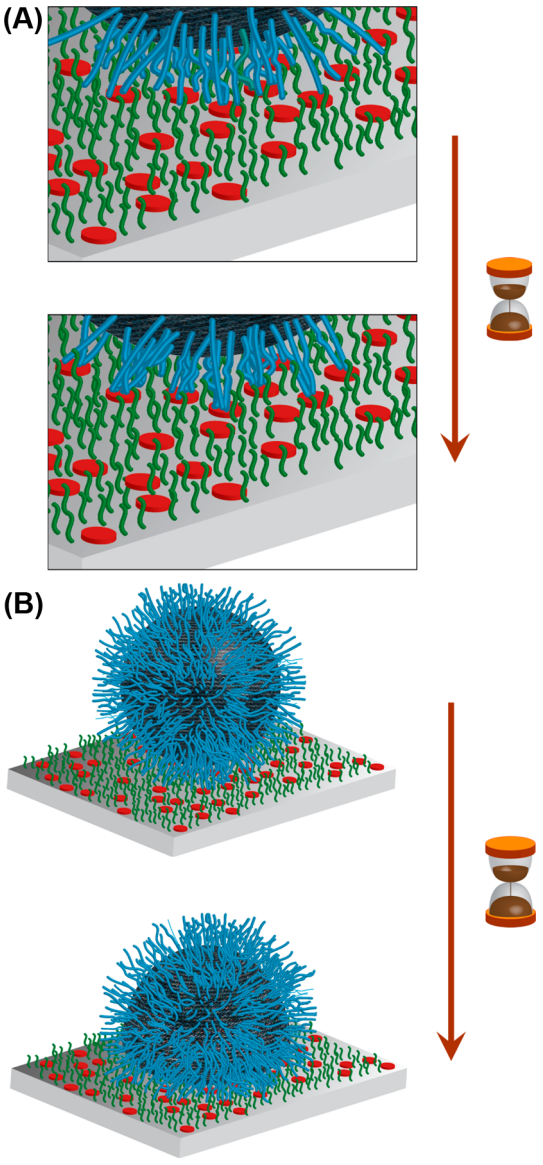

Figure 5. (A) A mechanism to increase bacteria adhesion strength, shown for the case of PLL-based adhesive nanoconstructs (represented as red disks) which, as indicated, are embedded in a repulsive polymer brush (represented by green strands). Adhesion is driven by electrostatic attractions in the region of existing "contact" and involving molecular-scale rearrangements of the contact region. The blue "bristles" represent molecules on the bacterial surface. (B) A mechanism to increase bacteria adhesion strength, shown for the case of PLL adhesive nanoconstructs (red disks) in a polymer brush (green line segments) and driven by electrostatic attractions outside the region of existing "contact" and involving deformation of the entire bacterium, analogous to droplet wetting.

constructs on the collector and the presentation of adhesive groups relative to the brush are surface design parameters controlling this mechanism.

Bacterial Spreading or "Wetting". In Figure 5B, a second potential mechanism for progressively increased bacterial adhesion after capture is the dynamic wetting of the collector by spreading bacteria. Such wetting processes involve continued bacteria deformation to increase contact area with the collecting surface, in a fashion resembling the spreading of a liquid droplet on a solid or the closing of a crack tip. It is the driving force for "wetting", occurring just outside the 3-phase bacterium-collector contact line, that distinguishes wetting from the mechanism of *local rearrangement* (whose driving force was within the existing contact area). That is, bacterial spreading will depend on the bacterial surface charge and its attraction, through a wedge-shaped water gap, to charges on the collector. Also important, bending resistance from a bacterium must be overcome by these adhesive interactions and can, as we have shown for vesicles, arrest spreading processes and lead to delayed responses.[47,48] The distribution of cationic nanoconstructs over the surface is therefore a critical design consideration in controlled bacterial, *via* the prevention of spreading. Ionic strength plays an additional role in spreading by determining the collector area, outside the instantaneous contact region, that is able to attract the bacterium.

The two mechanisms of local rearrangements and spreading, driven by interactions within and just beyond the contact region, respectively, are not mutually exclusive. Hence, the presentation of charge relative to the brush and its clustering, in addition to the local charge density, can all affect bacterial adhesion after capture.

CONCLUSIONS

This study examined the residence time dependence of *S. aureus* release from surfaces with broadly different presentations of attractive electrostatic charge. Compared with the literature which focused on short time bacteria–surface interactions during capture, our study emphasized longer surface residence times, on the order of tens of minutes, relevant to the cleaning of antimicrobial surfaces or on-line bacterial sensing. The study compared *S. aureus* release from surfaces sparsely functionalized with cationic chains and nanoparticles in a sterically repulsive polymer brush, to those with denser cationic functionality. Surfaces sparsely functionalized with different cationic constructs were chosen to give similar capture kinetics, and therefore similar initial *S. aureus* interactions. Then with the capture kinetics, and hence the average initial bacteria–surface interactions fixed, the subsequent evolution of adhesion was inferred from bacterial release in higher shear.

The study demonstrated how surfaces with appropriately designed charge densities and presentations can decouple the initial *S. aureus* binding from subsequent increases in bacterial adhesion strength. In particular, *S. aureus* captured on collectors with low levels of clustered charge were slow to progressively increase their adhesion strength. Also, with attractive functionality clustered on sparsely situated cationic nanoparticles, *S. aureus* adhesion strength was limited

to the low levels that occurred near the time of capture. Additional strengthening of bacterial adhesion was prevented on the sparse nanoparticle surfaces, enabling subsequent bacterial removal in elevated shear: easy come, easy go. On these surfaces, residence time, up to 30 min, had no effect on the forces needed to dislodge the previously bound bacteria.

Because *S. aureus* adhesion evolved differently on different surfaces at fixed ionic strength, and because the bacterial removal at fixed ionic strength depended on the ionic strength during aging, we are certain that the structure of the *S. aureus*–substrate interface evolves after bacterial capture. Two mechanisms (not mutually exclusive) were proposed for this evolution: closer approach of negative bacteria surface structures to cationic surface nanoconstructs and a more global increase in the bacteria–surface contact area involving large-scale bacterial deformation, like the spreading of a water droplet. The presentation of cationic charge on the surface relative to the repulsive PEG brush and the arrangement of the cationic charge in cluster on the substrate were identified as important design parameters affecting these mechanisms.

EXPERIMENTAL SECTION

Poly-L-lysine (PLL), having a nominal molecular weight of 20 000 and purchased from Sigma-Aldrich, was employed directly as a bacteria-adhesive cationic surface nanoconstruct. Cationically functionalized gold nanoparticles were also employed as adhesive surface nanoconstructs. These were synthesized as described previously,[49,50] and consisted of 7.5 nm gold cores with approximately 500 ligands per nanoparticle. Approximately 300 of the ligands were 1-mercaptoundecane and approximately 200 were *N*,*N*,*N*-trimethyl(11-mercaptoundecyl)-ammonium chloride, providing 200 cationic groups per nanoparticle. As a point of comparison, each PLL chain nominally contained 120 monomers, the ionization of which was pH-dependent. Near pH 7, most of these amines are positively charged.[51] Both individual PLL coils and cationic nanoparticles are ~10 nm in diameter, as determined by light scattering or TEM, respectively.

The same PLL was also used, separately, to anchor PEG chains to the surface and to position the sterically repulsive PEG brush around the preadsorbed PLL coils or nanoparticles. When PLL was used as the anchoring component of the PEG brush, it was first linked to amine-reactive PEG to form a bottle-brush or graft copolymer, as originally developed by Huang *et al.*[52] and Kenausis *et al.*[53] Our application requires brushes that do not adhere any proteins or bacteria.[40,43] We found a PLL backbone functionalization of 35% by 2000 molecular PEG to be appropriate. Notably, the functionalized PEG in the original references[52,53] was no longer available so we adopted a modified procedure,[40] in which the reaction of the *N*-hydroxysuccinimidyl ester of methoxypolyethylene glycol (Laysan Bio, Inc.) and the PLL was conducted in pH 9.1 carbonate buffer for 6 h prior to dialysis against pH 7.4 phosphate buffered saline.

This work compares 4 different surfaces, all on silica substrates. Microscope slides were acid etched overnight to produce the silica surface,[54] rinsed thoroughly in DI (deionized) water, and placed in a slit-shear flow chamber, and adsorbing species were deposited. Unless otherwise noted, adsorption was conducted from flowing pH 7.4 buffer (0.002 M KH_2PO_4 and 0.008 M Na_2HPO_4, having an ionic strength of 0.026 M and Debye length of 2 nm). The wall shear rate during deposition was 22 s^{-1}. The first surface was an adsorbed layer of PLL. This was formed by flowing a 5 ppm solution of PLL in buffer over the slide until the surface was saturated, producing an adsorbed PLL layer of about 0.4 mg/m^2. Buffer was then reinjected to clear away free PLL. A second densely functionalized surface was based on the cationic nanoparticles. Here nanoparticles at a concentration of 5 ppm in DI water were flowed over the surface until saturation, at about 1000 np/μm^2. DI water was subsequently reinjected to remove nanoparticles from the chamber.

Surfaces with relatively sparse random arrangements of adhesive nanoconstructs were produced by timed flow of solutions (5 ppm PLL in 0.026 M pH 7 buffer or 5 ppm nanoparticles in DI water), followed by reintroduction of buffer or DI water to stop adsorption short of saturation. These procedures adhered to our previous protocols,[38,40] which were based on quantitative reflectometry experiments that tracked of PLL or cationic nanoparticles adsorption, *in situ*. The success of this approach is ensured by the highly controlled and reproducible nature of transport-limited PLL and cationic nanoparticle adsorption kinetics.

After the adhesive nanoconstructs were deposited and the free solution was cleared of adsorbing cationic nanoconstructs, a 100 ppm solution of PLL-PEG in pH 7.4, 0.026 M phosphate buffer was reintroduced to backfill the PEG brush on the remaining surface. This PLL-PEG solution was allowed to flow until the surface was saturated, typically 10 min for the two sparse surface compositions. Finally, flowing buffer was reintroduced.

After surfaces were created, the bacteria portion of the study continued in the same slit flow chamber, on a custom optical microscope that orients the substrate perpendicular to the floor, avoiding the impact of gravity on bacteria–surface interactions. A 20× objective provided a large field of observation (240 μm × 180 μm) to accommodate monitoring large numbers of bacteria. *S. aureus* were deposited on the surfaces, from pH 7.4 buffer (having an ionic strength of 0.026 M and a Debye length of 2 nm) and a suspension concentration near 2 × 10^6 cells/mL, with a wall shear rate of 22 s^{-1}. The numbers of *S. aureus* on the surface, during deposition, aging, and shear challenge, were recorded on video, and later counted in different frames.

The *S. aureus* themselves, ATCC 25923, were grown in Luria–Bertani (LB) liquid medium, as is standard. Cultures were incubated overnight, shaking at 200 rpm at 37 °C, and then harvested after a total of 24 h during logarithmic growth. To remove proteins and other molecules that could potentially interfere with bacteria–surface interactions, suspensions were centrifuged at 1000*g* and cells subsequently resuspended in buffer. This washing procedure was repeated twice, and the final bacteria concentration, either 5 × 10^5/mL for studies of the capture efficiency in Figure 2 or 2 × 10^6/mL for rapid deposition prior to removal studies, was then formulated. Bacteria were stored at 4 °C and used within 24 h.

Bacteria viability was confirmed for each batch of *S. aureus* and at the beginning of adhesion runs, using a standard live/dead BacLight kit (Invitrogen, Carlsbad, CA). *S. aureus* bacteria were mixed with the dye mixture, incubated for 15 min, and then examined on a microscope slide on a Nikon Diaphot 300 inverted fluorescence microscope. Viewed under green (420–480 nm excitation/520–800 nm emission) and then red (480–550 nm excitation/590–800 nm emission) filters, viability was determined: viable bacteria appeared green while dead bacteria appeared red. Typically, bacterial suspensions were viable, presenting no more than 0.5% red-dead cells, with several hundred cells imaged in each field of view.

Because each batch of bacteria was employed in several sequential runs and calibrations, refrigerated bacterial storage at 4 °C with a total age of no more than 24 h (by the end of the last run) maintained bacteria in a resting state: bacteria counts of the initial suspensions and those used later revealed the same bacterial numbers within 10% during the 24 h period, also

evident in the quantitative reproducibility of the dynamic runs. (The bacterial capture rate, especially on the strongly cationic PLL surface, was transport limited and therefore quantitatively proportional to the numbers of suspended cells.) Reproducibility of capture kinetics ensured bacterial consistency and was, more importantly, a critical parameter in our experimental design. A targeted number of bacteria (~500 cells in the field of view) was reproducibly loaded onto each test surface in the targeted time window (3 min) so that the residence time of adhered bacterial (the main independent parameter in this study) could be quantitatively compared between samples and adhesion runs.

Finally, we were cautious to avoid changes in the bacteria during refrigerated storage. To this end, duplicate tests employed the freshest bacteria from the growth and purification, and a repeat run employing bacteria refrigerated for 18 h. These data, showing excellent reproducibility and arguing against any influence of refrigerated storage, are highlighted in Figure 3 of the results and are discussed in turn.

Conflict of Interest: The authors declare no competing financial interest.

Acknowledgment. This work was supported by the Center for Hierarchical Manufacturing at UMass, NSF 1025020.

REFERENCES AND NOTES

1. Hermansson, M. The DLVO Theory in Microbial Adhesion. *Colloid Surf., B* **1999**, *14*, 105–119.
2. Palmer, J.; Flint, S.; Brooks, J. Bacterial Cell Attachment, the Beginning of a Biofilm. *J. Ind. Microbiol. Biotechnol.* **2007**, *34*, 577–588.
3. Meinders, J. M.; vanderMei, H. C.; Busscher, H. J. Deposition Efficiency and Reversibility of Bacterial Adhesion under Flow. *J. Colloid Interface Sci.* **1995**, *176*, 329–341.
4. Vadillo-Rodriguez, V.; Busscher, H. J.; Norde, W.; de Vries, J.; van der Mei, H. C. Atomic Force Microscopic Corroboration of Bond Aging for Adhesion of *Streptococcus thermophilus* to Solid Substrata. *J. Colloid Interface Sci.* **2004**, *278*, 251–254.
5. Busscher, H. J.; van der Mei, H. C. How Do Bacteria Know They Are on a Surface and Regulate Their Response to an Adhering State?. *PLoS Pathog.* **2012**, *8*, e1002440.
6. van der Mei, H. C.; Rustema-Abbing, M.; de Vries, J.; Busscher, H. J. Bond Strengthening in Oral Bacterial Adhesion to Salivary Conditioning Films. *Appl. Environ. Microbiol.* **2008**, *74*, 5511–5515.
7. Younes, J. A.; van der Mei, H. C.; van den Heuvel, E.; Busscher, H. J.; Reid, G. Adhesion Forces and Coaggregation between Vaginal Staphylococci and Lactobacilli. *PLoS One* **2012**, *7*, e36917.
8. Boks, N. P.; Kaper, H. J.; Norde, W.; Busscher, H. J.; van der Mei, H. C. Residence Time Dependent Desorption of *Staphylococcus epidermidis* from Hydrophobic and Hydrophilic Substrata. *Colloid Surf., B* **2008**, *67*, 276–278.
9. Soumya, E.; Saad, I. K.; Abdellah, H.; Hassan, L. Experimental and Theoretical Investigations of the Adhesion Time of Penicillium Spores to Cedar Wood Surface. *Mater. Sci. Eng. C* **2013**, *33*, 1276–1281.
10. Wang, H.; Sodagari, M.; Chen, Y. J.; He, X.; Newby, B. M. Z.; Ju, L. K. Initial Bacterial Attachment in Slow Flowing Systems: Effects of Cell and Substrate Surface Properties. *Colloid Surf., B* **2011**, *87*, 415–422.
11. Xu, L. C.; Vadillo-Rodriguez, V.; Logan, B. E. Residence Time, Loading Force, pH, and Ionic Strength Affect Adhesion Forces between Colloids and Biopolymer-Coated Surfaces. *Langmuir* **2005**, *21*, 7491–7500.
12. Ploux, L.; Ponche, A.; Anselme, K. Bacteria/Material Interfaces: Role of the Material and Cell Wall Properties. *J. Adhes. Sci. Technol.* **2010**, *24*, 2165–2201.
13. Busscher, H. J.; Norde, W.; Sharma, P. K.; van der Mei, H. C. Interfacial Re-Arrangement in Initial Microbial Adhesion to Surfaces. *Curr. Opin. Colloid Interface Sci.* **2010**, *15*, 510–517.
14. Olsson, A. L. J.; van der Mei, H. C.; Busscher, H. J.; Sharma, P. K. Novel Analysis of Bacterium-Substratum Bond Maturation Measured Using a Quartz Crystal Microbalance. *Langmuir* **2010**, *26*, 11113–11117.
15. Boks, N. P.; Busscher, H. J.; van der Mei, H. C.; Norde, W. Bond-Strengthening in Staphylococcal Adhesion to Hydrophilic and Hydrophobic Surfaces Using Atomic Force Microscopy. *Langmuir* **2008**, *24*, 12990–12994.
16. Vanloosdrecht, M. C. M.; Lyklema, J.; Norde, W.; Zehnder, A. J. B. Influence of Interfaces on Microbial Activity. *Microbiol. Rev.* **1990**, *54*, 75–87.
17. Abu-Lail, N. I.; Camesano, T. A. Specific and Nonspecific Interaction Forces between *Escherichia coli* and Silicon Nitride, Determined by Poisson Statistical Analysis. *Langmuir* **2006**, *22*, 7296–7301.
18. Lin, J.; Qiu, S. Y.; Lewis, K.; Klibanov, A. M. Mechanism of Bactericidal and Fungicidal Activities of Textiles Covalently Modified with Alkylated Polyethylenimine. *Biotechnol. Bioeng.* **2003**, *83*, 168–172.
19. Murata, H.; Koepsel, R. R.; Matyjaszewski, K.; Russell, A. J. Permanent, Non-Leaching Antibacterial Surfaces - 2: How High Density Cationic Surfaces Kill Bacterial Cells. *Biomaterials* **2007**, *28*, 4870–4879.
20. Tiller, J. C.; Lee, S. B.; Lewis, K.; Klibanov, A. M. Polymer Surfaces Derivatized with Poly(vinyl-N-hexylpyridinium) Kill Airborne and Waterborne Bacteria. *Biotechnol. Bioeng.* **2002**, *79*, 465–471.
21. Tiller, J. C.; Liao, C. J.; Lewis, K.; Klibanov, A. M. Designing Surfaces that Kill Bacteria on Contact. *Proc. Natl. Acad. Sci. U. S. A.* **2001**, *98*, 5981–5985.
22. Kelly, A. M.; Kaltenhauser, V.; Muhlbacher, I.; Rametsteiner, K.; Kren, H.; Slugovc, C.; Stelzer, F.; Wiesbrock, F. Poly(2-oxazoline)-Derived Contact Biocides: Contributions to the Understanding of Antimicrobial Activity. *Macromol. Biosci.* **2013**, *13*, 116–125.
23. Qu, W. W.; Hooymans, J. M. M.; Qiu, J.; de-Bont, N.; Gelling, O. J.; van der Mei, H. C.; Busscher, H. J. Nonadhesive, Silica Nanoparticles-Based Brush-Coated Contact Lens Cases Compromising between Ease of Cleaning and Microbial Transmission to Contact Lenses. *J. Biomed. Mater. Res., Part B* **2013**, *101B*, 640–647.
24. Siedenbiedel, F.; Tiller, J. C. Antimicrobial Polymers in Solution and on Surfaces: Overview and Functional Principles. *Polymers* **2012**, *4*, 46–71.
25. Strauss, J.; Kadilak, A.; Cronin, C.; Mello, C. M.; Camesano, T. A. Binding, Inactivation, and Adhesion Forces between Antimicrobial Peptide Cecropin P1 and Pathogenic *E. coli*. *Colloid Surf., B* **2010**, *75*, 156–164.
26. Liu, Y.; Strauss, J.; Camesano, T. A. Adhesion Forces between *Staphylococcus epidermidis* and Surfaces Bearing Self-Assembled Monolayers in the Presence of Model Proteins. *Biomaterials* **2008**, *29*, 4374–4382.
27. Xie, X.; Moller, J.; Konradi, R.; Kisielow, M.; Franco-Obregon, A.; Nyfeler, E.; Muhlebach, A.; Chabria, M.; Textor, M.; Lu, Z. H.; Reimhult, E. Automated Time-Resolved Analysis of Bacteria-Substrate Interactions using Functionalized Microparticles and Flow Cytometry. *Biomaterials* **2011**, *32*, 4347–4357.
28. Rose, S. F.; Okere, S.; Hanlon, G. W.; Lloyd, A. W.; Lewis, A. L. Bacterial Adhesion to Phosphorylcholine-Based Polymers with Varying Cationic Charge and the Effect of Heparin Pre-Adsorption. *J. Mater. Sci.: Mater. Med.* **2005**, *16*, 1003–1015.
29. Chen, R. X.; Cole, N.; Willcox, M. D. P.; Park, J.; Rasul, R.; Carter, E.; Kumar, N. Synthesis, Characterization and *in Vitro* Activity of a Surface-Attached Antimicrobial Cationic Peptide. *Biofouling* **2009**, *25*, 517–524.
30. Madkour, A. E.; Dabkowski, J. A.; Nusslein, K.; Tew, G. N. Fast Disinfecting Antimicrobial Surfaces. *Langmuir* **2009**, *25*, 1060–1067.
31. Charnley, M.; Textor, M.; Acikgoz, C. Designed Polymer Structures with Antifouling-Antimicrobial Properties. *React. Funct. Polym.* **2011**, *71*, 329–334.
32. Cao, Z. Q.; Mi, L.; Mendiola, J.; Ella-Menye, J. R.; Zhang, L.; Xue, H.; Jiang, S. Y. Reversibly Switching the Function of a

Surface between Attacking and Defending against Bacteria. *Angew. Chem., Int. Ed.* **2012**, *51*, 2602–2605.
33. Cheng, G.; Xite, H.; Zhang, Z.; Chen, S. F.; Jiang, S. Y. A Switchable Biocompatible Polymer Surface with Self-Sterilizing and Nonfouling Capabilities. *Angew. Chem., Int. Ed.* **2008**, *47*, 8831–8834.
34. Jiang, S. Y.; Cao, Z. Q. Ultralow-Fouling, Functionalizable, and Hydrolyzable Zwitterionic Materials and Their Derivatives for Biological Applications. *Adv. Mater.* **2010**, *22*, 920–932.
35. Khoo, X.; Grinstaff, M. W. Novel Infection-Resistant Surface Coatings: A Bioengineering Approach. *MRS Bull.* **2011**, *36*, 357–366.
36. Lee, J.; Jung, J.; Na, K.; Heo, P.; Hyun, J. Polypeptide-Mediated Switchable Microarray of Bacteria. *ACS Appl. Mater. Interfaces* **2009**, *1*, 1359–1363.
37. Gon, S.; Kumar, K. N.; Nusslein, K.; Santore, M. M. How Bacteria Adhere to Brushy PEG Surfaces: Clinging to Flaws and Compressing the Brush. *Macromolecules* **2012**, *45*, 8373–8381.
38. Fang, B.; Gon, S.; Park, M.; Kumar, K. N.; Rotello, V. M.; Nusslein, K.; Santore, M. M. Bacterial Adhesion on Hybrid Cationic Nanoparticle-Polymer Brush Surfaces: Ionic Strength Tunes Capture from Monovalent to Multivalent Binding. *Colloid Surf., B* **2011**, *87*, 109–115.
39. Maddikeri, R. R.; Tosatti, S.; Schuler, M.; Chessari, S.; Textor, M.; Richards, R. G.; Harris, L. G. Reduced Medical Infection Related Bacterial Strains Adhesion on Bioactive RGD Modified Titanium Surfaces: A First Step toward Cell Selective Surfaces. *J. Biomed. Mater. Res., Part A* **2008**, *84A*, 425–435.
40. Gon, S.; Bendersky, M.; Ross, J. L.; Santore, M. M. Manipulating Protein Adsorption Using a Patchy Protein-Resistant Brush. *Langmuir* **2010**, *26*, 12147–12154.
41. Gon, S.; Santore, M. M. Single Component and Selective Competitive Protein Adsorption in a Patchy Polymer Brush: Opposition between Steric Repulsions and Electrostatic Attractions. *Langmuir* **2011**, *27*, 1487–1493.
42. Fang, B.; Gon, S.; Park, M. H.; Kumar, K. N.; Rotello, V. M.; Nusslein, K.; Santore, M. M. Using Flow to Switch the Valency of Bacterial Capture on Engineered Surfaces Containing Immobilized Nanoparticles. *Langmuir* **2012**, *28*, 7803–7810.
43. Gon, S.; Fang, B.; Santore, M. M. Interaction of Cationic Proteins and Polypeptides with Biocompatible Cationically-Anchored PEG Brushes. *Macromolecules* **2011**, *44*, 8161–8168.
44. Goldman, A. J.; Cox, R. G.; Brenner, H. Slow Viscous Motion of a Sphere Parallel to a Plane Wall. I. Motion through a Quiescent Fluid. *Chem. Eng. Sci.* **1967**, *22*, 653–659.
45. Kalasin, S.; Martwiset, S.; Coughlin, E. B.; Santore, M. M. Particle Capture *via* Discrete Binding Elements: Systematic Variations in Binding Energy for Randomly Distributed Nanoscale Surface Features. *Langmuir* **2010**, *26*, 16865–16870.
46. Duffadar, R.; Kalasin, S.; Davis, J. M.; Santore, M. M. The Impact of Nanoscale Chemical Features on Micron-Scale Adhesion: Crossover from Heterogeneity-Dominated to Mean-Field Behavior. *J. Colloid Interface Sci.* **2009**, *337*, 396–407.
47. Nam, J.; Santore, M. M. The Adhesion Kinetics of Sticky Vesicles in Tension: The Distinction between Spreading and Receptor Binding. *Langmuir* **2007**, *23*, 10650–10660.
48. Nam, J.; Santore, M. M. Depletion *versus* Deflection: How Membrane Bending Can Influence Adhesion. *Phys. Rev. Lett.* **2011**, *107*, 078101.
49. Srivastava, S.; Samanta, B.; Jordan, B. J.; Hong, R.; Xiao, Q.; Tuominen, M. T.; Rotello, V. M. Integrated Magnetic Bionanocomposites through Nanoparticle-Mediated Assembly of Ferritin. *J. Am. Chem. Soc.* **2007**, *129*, 11776–11780.
50. Zhang, J.; Srivastava, S.; Duffadar, R.; Davis, J. M.; Rotello, V. M.; Santore, M. M. Manipulating Microparticles with Single Surface-Immobilized Nanoparticles. *Langmuir* **2008**, *24*, 6404–6408.
51. Burke, S. E.; Barrett, C. J. pH-Responsive Properties of Multilayered Poly(L-lysine)/Hyaluronic Acid Surfaces. *Biomacromolecules* **2003**, *4*, 1773–1783.
52. Huang, N. P.; Michel, R.; Voros, J.; Textor, M.; Hofer, R.; Rossi, A.; Elbert, D. L.; Hubbell, J. A.; Spencer, N. D. Poly(L-lysine)-*g*-poly(ethylene glycol) Layers on Metal Oxide Surfaces: Surface-Analytical Characterization and Resistance to Serum and Fibrinogen Adsorption. *Langmuir* **2001**, *17*, 489–498.
53. Kenausis, G. L.; Voros, J.; Elbert, D. L.; Huang, N. P.; Hofer, R.; Ruiz-Taylor, L.; Textor, M.; Hubbell, J. A.; Spencer, N. D. Poly(L-lysine)-g-poly(ethylene glycol) Layers on Metal Oxide Surfaces: Attachment Mechanism and Effects of Polymer Architecture on Resistance to Protein Adsorption. *J. Phys. Chem. B* **2000**, *104*, 3298–3309.
54. Fu, Z. G.; Santore, M. M. Poly(ethylene oxide) Adsorption onto Chemically Etched Silicates by Brewster Angle Reflectivity. *Colloid Surf., A* **1998**, *135*, 63–75.